

Vibronic Effects in the $1^1B_u(1^1B_2)$ Excited Singlet States of Oligothiophenes. Fluorescence Study of the $1^1A_g(1^1A_1) \leftarrow 1^1B_u(1^1B_2)$ Transition in Terms of DFT, TDDFT, and CASSCF Methods

Marcin Andrzejak* and Marek T. Pawlikowski

Department of Theoretical Chemistry, Faculty of Chemistry, Jagiellonian University, 30-060 Kraków, Ingardena 3, Poland

Received: September 1, 2008; Revised Manuscript Received: October 21, 2008

A combined DFT/TDDFT approach has been applied for calculating the Huang–Rhys (HR) parameters along the totally symmetric normal coordinates for the $1^1A_g(1^1A_1) \leftarrow 1^1B_u(1^1B_2)$ electronic transition in a series of oligothiophenes containing from 2 to 6 thiophene rings. The calculations required optimized molecular geometries for both the ground state and the excited molecular state. The excited state geometry optimization was carried out by means of the time-dependent density functional theory (TDDFT) based methodology implemented in the Turbomole 5.9¹ package of programs. The results for the three smallest oligothiophenes were verified by generating the theoretical vibronic structures and comparing them with the high-resolution fluorescence spectra measured for matrix-isolated molecules. For bithiophene a comparison was also made of the theoretical results obtained for different basis sets and the most popular exchange–correlation functionals. The best results were then confronted with the HR parameters based on the molecular geometries calculated at the CASSCF level of theory. The results obtained within the DFT/TDDFT approach are in very good agreement with the available experimental data for bithiophene, terthiophene, and quaterthiophene molecules.

I. Introduction

Because of various potential applications in electronics, oligothiophenes have been extensively studied in an attempt to build a bridge between molecules and polymers. Quite easily soluble, forming neat single crystals, some of them even volatile enough to allow for gas phase experiments, the oligothiophene molecules are relatively easy to study as compared to polymers. At the same time, most of their properties can be extrapolated to describe polymeric materials. Initially, the works have been focused on small species (with 2–6 thiophene rings), which have not yet lost much of their popularity. However, larger oligomers (up to over twenty thiophene rings) have also entered the stage, owing to the widespread interest in organic electronics, and recently a number of devices built with oligothiophenes as key components have been presented.^{2–7} Because of the optoelectronic applicability a large portion of research has been directed toward the charge generating and charge transporting properties as well as the excitonic energy transport within the crystals. There are still vivid debates about the electronic structure of the oligomers. The disputes concern the nature of the intra- and intermolecular excited states, the importance of the electron–electron interactions, electron–vibronic and exciton–vibronic coupling, the mobilities of charges and excitons, etc.

The lowest energy excited singlets are the most easily probed states of thiophene oligomers. Owing to their high oscillator strengths, these states play a crucial role in the energy absorption and emission processes and in the energy transport within the crystal. The electronic structure of these states is rather simple, being represented mainly by a configuration corresponding to a single electron promotion from HOMO to LUMO. On

empirical grounds, the location of the lowest singlet states of oligothiophenes is now quite well established, even if the experiments were mostly done either in solution or in the matrix.^{8–12} The reported values of energies contain thus a contribution from the interactions between the molecule and environment. Successful supersonic jet experiments carried out for bithiophene¹³ have allowed for some estimate of this contribution. The excited state characteristics of oligothiophenes have also been subject to a few theoretical studies within semiempirical^{9,14–18} and ab initio schemes.^{19–23} The computed energies and transition dipole moments were found to be in good agreement with the experimental data. At this stage, however, determination of the excited state geometries presents a challenge, especially if one aspires to go beyond semiempirical treatment. The results of CASSCF computations²⁴ have been recently reported and analyzed for bithiophene. Nevertheless, to the best of our knowledge, the results of ab initio computations for terthiophene, and other members of the oligothiophene family, have not been reported yet, supposedly because of the excessively large active space necessary for reliable CASSCF computations. Moreover, it is not a simple matter to experimentally verify the computational results as the excited state geometries are not easily measurable for molecules containing more than several atoms. Some limited, yet essential, information about the excited state geometries can be gained from high-resolution UV–Vis absorption or fluorescence spectra. These spectra show more or less resolved vibronic structures, predominately due to the activity of totally symmetric oscillations. Theoretical analysis of these structures, however, is not straightforward as it requires in principle high-quality molecular geometries and normal modes for both the ground and the excited electronic states. Nevertheless, if the molecular geometry change upon electronic transition is not too large, and the respective normal modes for the electronic states involved in

* To whom the correspondence should be addressed. E-mail: andrzejka@chemia.uj.edu.pl.

the absorption/emission processes are likely to be similar, then the task can be reduced to a simple Franck–Condon (FC) analysis. In the framework of that analysis, the geometry differences are projected onto the normal coordinates of the ground state.^{14,25,26} The results of these projections, i.e., FC parameters, enter the vibrational overlap integrals which mediate in the intensity of an electronic transition and give rise to Poisson-like vibrational progressions in the absorption/emission spectra. Such a simple approach was successfully employed to elucidate the vibronic structures observed in the UV–Vis absorption and emission,²⁷ the magnetic circular dichroism (MCD),²⁸ and the resonance Raman²⁹ spectra of the small, medium, and large size molecules.

The vibronic couplings in general and the FC effect in particular are responsible not only for the intensity distributions observed in the absorption and emission spectra of isolated molecules. They also play a crucial role when studying the transport and relaxation phenomena in the solid states and crystals. In the excited electronic states of oligothiophenes, the vibronic effects have already been subject to both experimental^{11,13,30–32} and theoretical^{14,33–35} studies. Hence, the values of the FC parameters in the $1^1B_u(1^1B_2)$ state were roughly evaluated for the most prominent normal modes active in the oligothiophenes spectra.¹¹ Nevertheless, an in-depth analysis of the vibronic couplings in the lowest excited singlet state of oligothiophenes still calls for further studies, especially when the issue concerns the intensity distributions in the fluorescence spectra measured for the bi-, ter-, and quaterthiophene molecules embedded in the hydrocarbon matrices.

In this paper we present the FC analysis for the $1^1A_g(1^1A_1) \leftarrow 1^1B_u(1^1B_2)$ transition in oligothiophenes which contain 2–6 rings. This analysis has been done by means of density functional theory (DFT), with the time-dependent (TDDFT) approach employed to determine the excited state geometries of oligothiophenes studied. Being DFT based, the TDDFT approach offers the possibility of tackling much larger systems than other methods such as CASSCF or CASPT2. The appropriate numerical procedures available from new implementation of the Turbomole 5.9 package¹ have been used for our purposes. Since the implementation of the TDDFT approach is still fresh we have decided to examine the performance of this method using the opportunity offered by the high-resolution vibronic spectra available for oligothiophenes.^{30–32} For the bithiophene molecule we have tested the sensitivity of the computational results to the choice of the basis set and the exchange-correlation functional in TDDFT treatment. Also, a comparison has been made with the results of the CASSCF and CASPT2 calculations. Eventually, we generate the theoretical vibronic spectra and compare them to the experimental fluorescence spectra measured for bi-, tri-, and tetrathiophene molecules isolated in the hydrocarbon matrix.

II. 1^1A_g and 1^1B_u State Geometries

The X-ray diffraction experiments prove that the oligothiophenes in crystalline environment are flat or almost flat and every molecule has all-trans C_{2h} or C_{2v} symmetries depending on whether the number of thiophene rings is even or odd, respectively.^{36–40} Our computations in vacuum also showed that planar conformation corresponds to the genuine minimum on the potential energy surface (PES) for the lowest excited $1^1B_u(1^1B_2)$ singlet state of all the investigated oligothiophenes. On the other hand, the ground state vibrational analysis done under C_{2h} and/or C_{2v} symmetry constrains led us to imaginary frequencies. These correspond to the low-frequency out-of-plane

modes engaging the inter-ring torsional movements. Apparently, the true minimum on the ground state PES corresponds to conformations in which the adjacent thiophene rings are slightly twisted with respect to one another. Indeed, previously reported calculations for bithiophene^{21,41} as well as our DFT computations yielded the inter-ring dihedral angle of about 155° . Moreover, we checked that a deviation from planarity lowers the energy of the 1^1A_g state by less than 1 kcal/mol, indicating an extremely low curvature of the potential energy surface in the direction of the inter-ring rotation. This observation supports an earlier suggestion that even weak van der Waals interactions within the crystal are sufficient to enforce the planarity of the oligothiophene molecules.^{37–40} With the gas-to-solvent shift reaching for bithiophene nearly 0.2 eV,¹³ the guest–host interactions are strong enough to keep the molecular C_{2h} (or C_{2v}) conformation intact upon the transition between the $1^1A_g(1^1A_1)$ and $1^1B_u(1^1B_2)$ states, as indicated by the absence of the inter-ring torsion activity in the experimental spectra measured in the matrices. At this stage, the natural question arises what is the nuclear conformation of the oligothiophenes trapped in hydrocarbon matrices, for which the high-resolution spectra were recorded.^{30–32}

Whether the molecules embedded in the matrices are actually planar is difficult to determine. To this end, however, an assumption has to be done to make the problem tractable for purposes of theoretical analysis. Ergo, the computations can be performed either by keeping the molecules planar with the help of the imposed high symmetry or, should the conformation be twisted, by freezing out the inter-ring dihedral angle at a certain value. Since we had no way of telling what the actual value of the dihedral angle is, we opted for the former approach, which guaranteed that at least for the excited state we dealt with the genuine minimum on the PES. At this level of approximation, the activity of the totally symmetric modes observed in the emission and absorption spectra can be characterized in terms of Huang–Rhys (HR) factors $S_i = B_i^2/2$. These are referred to FC parameters B_i , which can be evaluated in the standard way^{14,25} from the formula

$$B_i = \left(\frac{\omega_i}{\hbar} \right) \cdot [\mathbf{x}_A - \mathbf{x}_B] \mathbf{M}^{1/2} \mathbf{L}_i^A \quad (1)$$

\mathbf{x}_A and \mathbf{x}_B are the $3N$ -dimensional vectors of the equilibrium Cartesian coordinates in the A th and B th states, \mathbf{M} is the $3N \times 3N$ diagonal matrix of the atomic masses, and \mathbf{L}_i^A is the $3N$ vector of the mass-weighted Cartesian displacements constituting the i th normal coordinate calculated for the A th (ground) electronic state.

In subsequent sections, eq 1 is applied to evaluate the FC parameters based on the results of the TDDFT calculations that provided the ground and the excited state geometries and normal mode coordinates of totally symmetric oscillations. To avoid complications, no attempt was made to include the rotation of totally symmetric modes due to a possible Dushinsky mode-mixing. At this level, the FC overlap integrals required to simulate the experimental spectra can be easily determined in the standard fashion from the well-known recursion formulas given elsewhere.⁴²

III. Computational Details

A. Bithiophene. As the smallest member of the oligothiophene family, bithiophene was used as a molecular model to test the methodology, to find out the optimum exchange-correlation functional, and to select a suitable basis set for our purposes. Initially, we chose extended, triple- ζ and quadruple- ζ

TABLE 1: Vibrational Frequencies and HR Parameters for the Totally Symmetric Normal Modes of Bithiophene, Calculated with a Series of Popular Exchange-Correlation Functionals Using the TZVP⁴³ Basis Set

	VWN		BP		BLYP		B3LYP		exptl ^a	
	$\bar{\nu}$ [cm ⁻¹]	<i>S</i>	$\bar{\nu}$ [cm ⁻¹]	<i>S</i>	$\bar{\nu}$ [cm ⁻¹]	<i>S</i>	$\bar{\nu}$ [cm ⁻¹]	<i>S</i>	$\bar{\nu}$ [cm ⁻¹]	<i>S</i>
1	290.6	0.13	282.6	0.06	278.1	0.03	289.4	0.10	298	0.36
2	375.7	0.44	371.6	0.41	371.1	0.41	381.9	0.43	391	0.45
3	679.2	0.66	663.2	0.70	653.6	0.71	680.6	0.67	682	0.38
4	740.3	0.18	719.1	0.17	702.1	0.18	737.4	0.25	752	0.28
5	854.3	0.00	835.4	0.00	825.4	0.01	857.0	0.00		
6	1042.3	0.03	1046.7	0.02	1044.9	0.02	1072.5	0.05		
7	1060.3	0.03	1070.6	0.05	1075.0	0.05	1107.0	0.06		
8	1176.0	0.00	1196.0	0.01	1176.7	0.02	1227.9	0.01		
9	1254.7	0.01	1240.6	0.01	1245.3	0.00	1282.2	0.00		
10	1372.9	0.00	1359.9	0.00	1354.9	0.00	1398.9	0.00		
11	1478.6	0.33	1444.5	0.42	1427.1	0.48	1483.5	0.66	1455	0.78
12	1583.1	0.23	1541.6	0.17	1525.6	0.14	1589.9	0.26	1569	0.55

^a Reference 31.**TABLE 2: Vibrational Frequencies and Huang–Rhys Parameters for the Totally Symmetric Normal Modes of Bithiophene**

	B3LYP (TZVP)		B3LYP (QZVP)		CASSCF (ANO-S)		CASSCF(ANO-S)/B3LYP(QZVP)		exptl ^a	
	$\bar{\nu}$ [cm ⁻¹]	<i>S</i>	$\bar{\nu}$ [cm ⁻¹]	<i>S</i>	$\bar{\nu}$ [cm ⁻¹]	<i>S</i>	$\bar{\nu}$ [cm ⁻¹]	<i>S</i>	$\bar{\nu}$ [cm ⁻¹]	<i>S</i>
1	289.4	0.10	291.9	0.19	282.3	0.61	291.9	0.58	298	0.36
2	381.9	0.43	380.2	0.50	370.3	0.00	380.2	0.00	391	0.45
3	680.6	0.67	684.7	0.68	661.2	0.16	684.7	0.17	682	0.38
4	737.4	0.25	749.9	0.23	729.4	0.51	749.9	0.47	752	0.28
5	857.0	0.00	864.3	0.00	836.9	0.00	864.3	0.00		
6	1072.5	0.05	1073.3	0.05	1028.4	0.02	1073.3	0.02		
7	1107.0	0.06	1102.1	0.07	1083.3	0.14	1102.1	0.12		
8	1227.9	0.01	1229.6	0.02	1219.9	0.01	1229.6	0.03		
9	1282.2	0.00	1282.8	0.00	1267.6	0.01	1282.8	0.00		
10	1398.9	0.00	1402.6	0.01	1376.9	0.02	1402.6	0.05		
11	1483.5	0.66	1472.5	0.63	1467.3	1.04	1472.5	0.97	1455	0.78
12	1589.9	0.26	1579.6	0.26	1572.4	0.31	1579.6	0.25	1569	0.55

^a Reference 31.

split valence basis sets augmented with polarization functions (TZVP,⁴³ QZVP⁴⁴). A series of exchange-correlation functionals, i.e., the local spin density Vosco–Wilk–Nusair (VWN),⁴⁵ the nonlocal spin density Becke–Perdew (BP),^{46,47} and the Becke’s nonlocal and hybrid approaches with Lee–Yang–Parr correlation functionals (BLYP,^{46,48} B3LYP^{46,49}), were applied. For each of the functionals chosen we found optimized geometries for the ground state (1^1A_g) and the lowest excited singlet state (1^1B_u). Subsequent vibrational analysis showed that the planar conformation indeed corresponds to the genuine minimum on the PES for the excited state, while among the ground state normal modes the inter-ring torsion had an imaginary frequency of about $i32$ cm⁻¹ (for all the functionals), indicating that for the ground state the planar conformation represents a first-order saddle point, in accordance with the results of Duarte et al.²¹ For all the functionals, however, the computed frequencies of the totally symmetric vibrations (see Table 1) are in excellent agreement with the experimental values measured for the matrix-isolated molecules. This supports our viewpoint that the results obtained for the planar conformation enforced in the calculations may be applied for description of bithiophene molecules entrapped in the hydrocarbon matrix.

The main directions of the geometry relaxation, indicated by large values of the HR parameters, are roughly the same for all functionals. Significant values of HR constants are found for four lowest energy totally symmetric vibrations (ν_1 – ν_4) and for two highest energy ones (ν_{11} , ν_{12}). The activities of these vibrations dominate the absorption/emission spectra, as was already noticed by Birnbaum and Kohler.³¹ The vibration at 1455 cm⁻¹ (ν_{11}) is particularly important. With the frequency only

slightly dependent on the number of thiophene rings, the ν_{11} mode is responsible for the most prominent vibronic progression in the $1^1A_g \rightarrow 1^1B_u$ band. This progression can also be recognized in the low-resolution spectra of other oligothiophenes. Analysis of those experimental data gave us a rough estimation of the corresponding HR parameters, which vary from $S_{11} = 1.06$ for terthiophene to $S_{11} = 0.80$ for sexithiophene.¹¹ The displacements obtained from our analysis (see Table 1) are slightly too small as compared to those extracted from absorption/emission experiments. However, of the four functionals applied for our purpose, the B3LYP/TZVP approach clearly behaves better than the others as long as the HR parameters are the same. Since the B3LYP functional leads also to the best estimation of the adiabatic excitation energy, which is only 6% lower than the experimental value,¹³ we decided that the hybrid B3LYP functional should be used in the course of further analysis. We wish to note the TZVP basis set employed in our computations offers a reasonable compromise between the quality of results and the time economy. We also checked that the B3LYP computations done with an enlarged QZVP basis brought about rather marginal modifications of the HR parameters, as can be seen in Table 2. The only noticeable difference could be detected for the ν_1 mode. The observed change in S_1 could probably lead to a somewhat better agreement with the experiment. Unfortunately, the increase of computational cost brought about by enlarging the basis set to QZVP was such that the calculations would require an abnormally long time for medium and large molecules. Therefore, for the other oligothiophenes studied in subsection B we were compelled to apply the TZVP basis set.

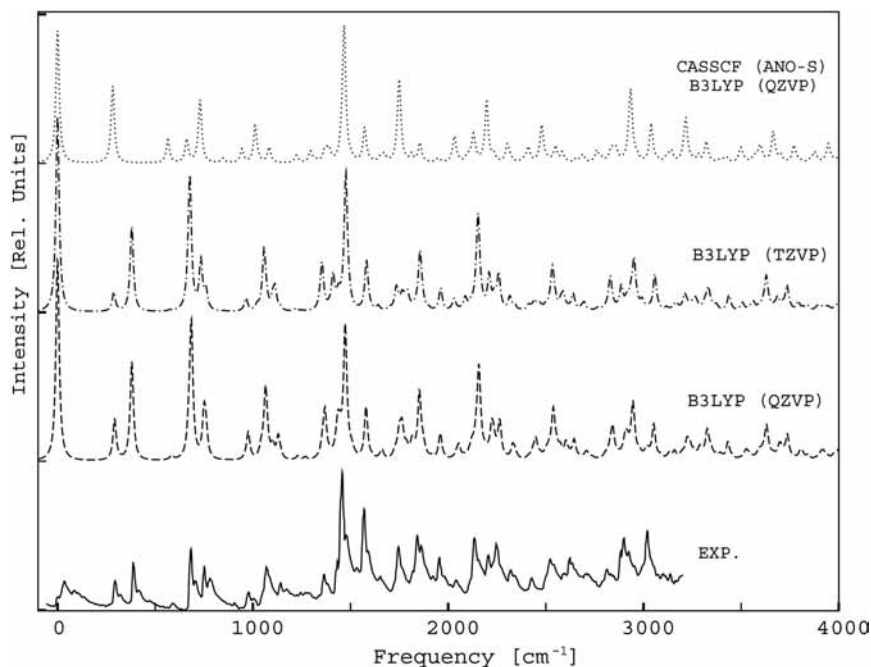


Figure 1. The experimental³¹ (solid line) and theoretical fluorescence spectra of bithiophene (2T). The theoretical structures were calculated at different levels of theory (the respective HR parameters are given in Table 2), using Lorentzians with $\text{fwhm} = 2 \text{ cm}^{-1}$ to create individual bands. The uppermost spectrum (dotted line) was obtained from a combined CASSCF/DFT approach (see the text).

To control the quality of DFT results, the HR parameters were also calculated for comparative purposes by means of CASSCF approach using the Molcas 6.4 package.⁵⁰ The molecular geometry of bithiophene was optimized for both the ground and the lowest excited singlet states, and the active space for 10 valence π orbitals occupied by 12 electrons was constructed. The ANO-S basis set⁵¹ was employed in the CASSCF computations. The quality of this approximation was verified on the basis of the CASPT2 vertical energy evaluations. The computations provide the vertical excitation energy of the 1^1B_u state to be 3.99 eV, in very good agreement with the value 3.86 eV acquired from the experiment.¹³ Also, the oscillator strength of 0.37 achieved for the $1^1\text{B}_u \rightarrow 1^1\text{A}_g$ transition looks very reasonable, being consistent with the value 0.42 predicted by the TDDFT method. At the CASSCF level, we were able to calculate both the geometries and the normal modes, whereas in the CASPT2 approach only the molecular geometries were available. Therefore, following an earlier paper of the field,⁵² we also challenged the “mixed approach” in which the geometries from CASSCF and the normal modes from DFT are combined in the single computational scheme. The HR parameters calculated in this way are also listed in Table 2. As follows from the comparison, the HR parameters obtained from the CASSCF geometries the two sets of normal modes are very similar to each other. This suggests that the quality of normal coordinates is not critical as far as the HR parameters in the 1^1B_u state of bithiophene are concerned. However, a closer inspection of Table 2 shows that HR parameters based on the CASSCF geometries are quite different from those obtained in the DFT (TDDFT) approach, especially in the low-energy region. Apparently the changes in the relative HR parameters are brought about by differences in the geometrical structures of the 1^1A_g and 1^1B_u states acquired from the CASSCF and DFT methods. However, we refrain here from further analysis of the molecular geometries of bithiophene obtained in the two approaches as it will be addressed in detail in the following paper that is currently in preparation.

In Figure 1 we present the experimental fluorescence spectrum (solid line) corresponding to the $1^1\text{A}_g \rightarrow 1^1\text{B}_u$ transition in the bithiophene molecule.³¹ For the sake of simplicity, the energy scale was shifted so that the zero on the abscissa corresponds to the 0–0 line of the adiabatic energy transition at 29603 cm^{-1} . Due to the self-absorption problem, the 0–0 band in the experimental spectrum is subject to substantial intensity reduction. Thus, the theoretical spectra were arbitrarily normalized to guarantee the band-to-band reproduction of the ν_{11} -fundamental of the bithiophene mode. The dashed and dot-dashed lines in Figure 1 give samples of the fluorescence spectra calculated with displacement FC parameters achieved within B3LYP/QZVP and B3LYP/TZVP treatments. For a comparison, the dotted line in Figure 1 shows the theoretical fluorescence calculated within the “mixed” approach, i.e., the geometry difference $\mathbf{x}_A - \mathbf{x}_B$ in eq 1 computed within CASSCF/ANO-S approach was projected on the normal coordinates taken from B3LYP/TZVP treatment.

Looking at Figure 1 we can easily notice that the purely DFT-based intensity patterns match very well the experimental fluorescence spectrum measured for bithiophene embedded in the matrix. The vibronic structure generated on the basis of the CASSCF results, however, is clearly inferior as compared to that of B3LYP/TZVP. In fact, an inspection of Figure 1 reveals that the empirical intensity pattern is rather poorly reproduced in the low-energy range from 200 to 700 cm^{-1} . Therefore, it is so also for the rest of the spectrum, which contains the combination bands of the low- and high-frequency modes. On the other hand, the B3LYP/TZVP-based vibronic structure appears to be free of drastic imperfection, even though the overall intensity in the low-energy region seems to be overestimated. Unfortunately, an insight in the vibronic structure of this region may be seriously limited also by the experimental conditions that could reduce the intensities of bands lying relatively close to the 0–0 line. This supposition is supported by the supersonic jet spectrum of bithiophene,¹³ which is very similar to the matrix isolated one, except for the low-energy

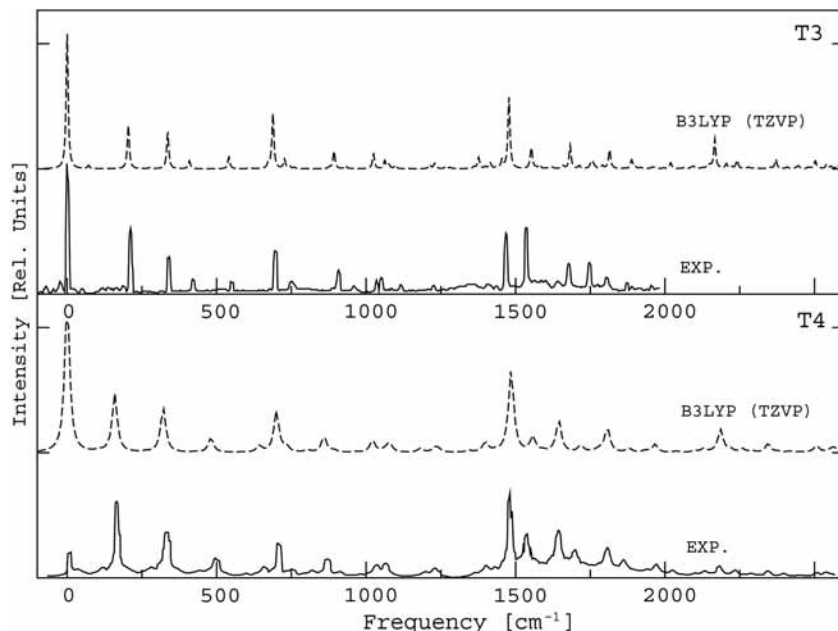


Figure 2. The experimental (solid line) and theoretical (dashed line) fluorescence spectra of terthiophene (3T, top)³⁰ and quaterthiophene (4T, bottom).³²

TABLE 3: Vibrational Frequencies and Huang–Rhys Parameters for the Selected Totally Symmetric Normal Modes of Oligothiophenes Containing 3–6 Thiophene Rings

	T3				T4				T5		T6	
	calcd		exptl		calcd		exptl		$\bar{\nu}$ [cm ⁻¹]	S	$\bar{\nu}$ [cm ⁻¹]	S
	$\bar{\nu}$ [cm ⁻¹]	S	$\bar{\nu}$ [cm ⁻¹]	S	$\bar{\nu}$ [cm ⁻¹]	S	$\bar{\nu}$ [cm ⁻¹]	S				
1	72.4	0.02			105.2	0.01			120.08	0.10	105.46	0.35
2	206.6	0.32	209.8	0.50	159.1	0.39	162	0.50	135.48	0.33	143.78	0.09
3	339.8	0.27	338.2	0.28	322.4	0.22	327	0.21	312.72	0.20	291.84	0.01
4	695.2	0.41	694.2	0.32	700.1	0.27	703	0.25	702.26	0.21	307.75	0.20
5	734.3	0.07			730.2	0.03			728.03	0.02	703.44	0.17
6	1073.0	0.04			736.5	0.01			735.27	0.01	726.74	0.01
7	1087.1	0.03			1073.1	0.04			1073.07	0.04	1073.14	0.05
8	1225.2	0.03			1082.2	0.03			1079.52	0.04	1077.96	0.04
9	1246.8	0.01			1223.5	0.02			1220.81	0.01	1218.33	0.01
10	1469.8	0.06			1233.1	0.01			1229.28	0.02	1227.77	0.02
11	1493.0	0.53	1462.3	0.45	1245.4	0.01			1240.02	0.01	1235.21	0.01
12	1568.7	0.15	1530.6	0.50	1470.2	0.02			1469.75	0.01	1472.17	0.52
13					1485.7	0.54	1478	0.55	1478.01	0.52	1488.27	0.02
14					1557.6	0.08	1531	0.17	1488.39	0.02	1547.01	0.03
15									1551.21	0.04		

region where it is evidently more intense, resembling thus the DFT-based theoretical structure. The DFT results reported in this study are also confirmed by crude estimates of the displacement parameters based on the high-energy region of the experimental spectrum (above the ν_{11} fundamental). Although the agreement is not perfect, especially for S_1 , S_3 , and S_{12} (Table 2), one should bear in mind that the values of the HR parameters based on the analysis of the peak heights in the experimental spectrum may also suffer from considerable inaccuracy. Therefore, dealing with the long oligothiophenes in the subsequent section we will refrain from a detailed comparison of the specific parameters and we will emphasize the good match between the theoretical and experimental spectra. We believe that the results obtained for bithiophene lend credit to the TDDFT as the method for finding geometries of the molecules in their excited states. We will seek further verification of this conjecture analyzing the results for larger oligothiophenes.

B. Oligothiophenes Containing 3–6 Thiophene Rings.

With the results for bithiophene described in subsection A we can now proceed to examine the fluorescence spectra of the molecules with three and more thiophene rings. In Figure 2 we give the experimental fluorescence spectra (solid lines) measured for the $1^1A_1 \leftarrow 1^1B_2$ and $1^1A_g \leftarrow 1^1B_u$ transitions of ter- and quaterthiophene, respectively. The theoretical simulations of these spectra presented as dashed lines in Figure 2 were achieved by using the TDDFT approach at the B3LYP/TZVP level of theory. The HR parameters used in the calculations are collected in Table 3.

A look at Figure 2 allows us to state that the agreement between the theory and the experiment is very good, even if some imperfections do appear, probably indicating the limitations of the vibronic model based solely on the simple FC approach. The major deviations from experiment can be noticed in the highest energy region of the fluorescence spectrum of terthiophene, especially around 1500 cm⁻¹. In this region, two fundamental lines of 1493 (ν_{11}) and 1568 cm⁻¹ (ν_{12}) modes build

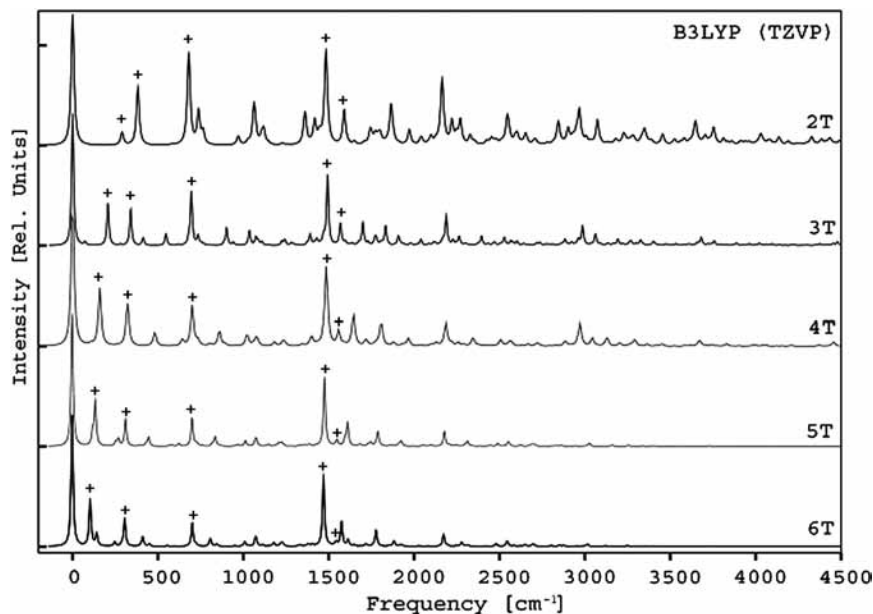


Figure 3. Theoretical fluorescence spectra calculated in the framework of DFT/TDDFT combined approach at the B3LYP/TZVP level of theory for bithiophene (2T), terthiophene (3T), quaterthiophene (4T), quinquethiophene (5T), and sexithiophene (6T). The relevant parameters are listed in Table 3. The five fundamental lines of the dominate the spectra are marked with a plus sign (+).

up the intensity distribution. The calculated intensity ratio $I(\nu_{11})/I(\nu_{12}) = 3.5$ is apparently too large as compared to the ratio of ca. 0.9 extracted from the experiment. In an attempt to understand this drawback it is conceivable to consider that the TDDFT treatment at the B3LYP/TZVP level underestimates the HR parameter of the 1568 cm^{-1} (ν_{12}) mode leading to the envisaged problem. However, it is also plausible that the totally symmetric normal coordinates are not identical in the electronic states involved in the fluorescence process. Specifically, not only FC but also mode-mixing (Dushinsky) effects can mediate the intensity distributions in the absorption and fluorescence spectra. In fact, assuming for simplicity that $\nu_{11} \cong \nu_{12}$ and applying the arguments presented elsewhere,⁵³ we could get an approximate but analytical expression:

$$\frac{I(\nu_{11})}{I(\nu_{12})} \cong \frac{(B_{11} \cos \phi + B_{12} \sin \phi)^2}{(B_{11} \sin \phi - B_{12} \cos \phi)^2} \quad (2)$$

in which ϕ is related to the rotation (mode-mixing) of ν_{11} and ν_{12} vibrations. For $\phi = 0$, expression 2 reduces to the equation $I(\nu_{11})/I(\nu_{12}) = (B_{11}/B_{12})^2$ known from the simple vibronic FC model employed in this paper. On the other hand, for $\phi \neq 0$ it is easy to show that the appropriate value of the intensity ratio $I(\nu_{11})/I(\nu_{12})$ can be reached when admitting the rotation of ν_{11} and ν_{12} modes. At this stage, it is reasonable to deliberate that the rotation of totally symmetric coordinates may be a factor when attempting to refine the fluorescence spectra, at least for terthiophene.

While the theoretical fluorescence spectra for the bi-, ter-, and quaterthiophene molecules could be directly verified on the experimental base, the high-resolution fluorescence spectra for the quinque- and sexithiophene have not been as yet reported. Nevertheless, it is still possible to look for distinctive spectroscopic features that can occur at the high-resolution fluorescence spectra of oligothiophenes, especially when a number of thiophene rings grows. A few such features can be immediately observed in Figure 3, where the calculated fluorescence spectra for the bi-, ter-, quater-, quinque-, and sexithiophene molecules are put together. All these spectra differ in details, but the

intensity distributions show roughly the same intensity patterns built essentially by a few vibrational modes of similar character. A closer look at Figure 3 allows us to notice, however, that the vibrational structures of these spectra become gradually more and more featureless at the higher energy site of the spectra, i.e., the intensities of the vibronic bands decrease faster as their energy increases.

These changes in the fluorescence spectra are associated with an alteration of molecular relaxation energy, E_{rel} , which is defined as a sum of the Huang–Rhys parameters multiplied by the respective oscillation energy quanta. We could check that the relaxation energy of the molecules studied can be, to very good approximation, evaluated from the expression: $E_{\text{rel}} = 7700.0(n^{-1} - 0.78n^{-2})$, n being the number of thiophene rings. Such a behavior resembles the one recognized in solid state physics, especially in the field of molecular crystals, when the intramolecular excitation is delocalized over a number of molecules (within so-called coherence distance). In such a case the relaxation energy decreases proportionally to the reciprocal of the number of molecules sharing the excitation. The spectroscopic consequence is, of course, the reduction of vibronic activity of the intramolecular oscillations, much like in the oligothiophenes. If the coherence distance is very large (as in very high-quality crystals in low temperature), only a single 0–0 line may remain. At present it is not easy to say whether the fluorescence spectra of very long oligothiophenes will also show similar behavior. In particular, it is difficult to state whether the vibronic structure would disappear so completely from the spectra of oligothiophenes larger than those examined in this paper. However, in the cases of quinquethiophene and sexithiophene molecules, we do hope that our theoretical prediction can, and will be verified soon by means of the high-resolution fluorescence experiments.

Returning to vibronic structures in Figure 3, we can distinguish five modes that dominate the spectra for all the investigated oligothiophenes. The fundamentals of these five modes referred further as I–V are marked by a plus sign (+) in Figure 3. Their frequencies and the corresponding HR parameters are collected in Table 4 for all oligothiophene studied. Going from

TABLE 4: The Frequencies and HR Parameters for the Most Prominent Totally Symmetric Modes of: bithiophene (2T), Terthiophene (3T), Quaterthiophene (4T), Quinquethiophene (5T), and Sexithiophene (6T)

		2T	3T	4T	5T	6T
mode I	freq [cm^{-1}]	289	207	159	135	105
	HR	0.10	0.32	0.39	0.33	0.35
mode II	freq [cm^{-1}]	382	340	322	313	307
	HR	0.43	0.27	0.22	0.20	0.20
mode III	freq [cm^{-1}]	681	695	700	702	703
	HR	0.67	0.41	0.27	0.21	0.17
mode IV	freq [cm^{-1}]	1484	1493	1486	1478	1472
	HR	0.66	0.53	0.54	0.52	0.52
mode V	freq [cm^{-1}]	1590	1569	1558	1551	1547
	HR	0.26	0.15	0.08	0.04	0.03

short to longer molecules, we can easily notice that the largest and systematic drop of frequency happens for the lowest energy mode I, which stretches the molecule in the direction of the long molecular axis. At the same time, the values of respective HR parameters obtained within the B3LYP/TZVP approach are quite similar, even if the bithiophene may be viewed as an exception. The departure from regularities for the low-frequency mode I of the bithiophene may be in part due to sensitivity of our computations on the enforced planarity of the molecules studied. The same applies for mode II for which the frequency 681 cm^{-1} and HR parameter 0.67 found for the bithiophene molecule stand out from these achieved for ter-, quarter-, quinque-, and sexithiophene molecules. On the other hand, frequencies of the two high-frequency modes IV and V that consist mainly of the stretches of the nominally single and double C–C bonds within the carbon skeleton of the molecules are rather unaffected by the growing size of the molecule. Concurrently, the variations of HR parameters for the ter-, quarter-, quinque-, and sexithiophene molecules are marginal for mode IV but not for mode V. For the latter, the calculated HR parameters systematically decrease when the size of oligothiophene grows. Eventually, let us address the problem of activity of the mode II and III in the fluorescence spectra of oligothiophenes. These modes can be characterized by the out-of-phase motions of nuclei along the ring symmetry axes and by the in-phase ring breathing plus S–C stretching. In these movements the all thiophene rings in the molecule oscillate with more or less the same amplitudes. Therefore, the HR parameters for vibrations II and III should be relatively insensitive on elongation of the oligothiophene chain. This can indeed be noticed when viewing the numerical data for the terthiophene, quaterthiophene, quinquethiophene, and sexithiophene molecules (Table 4). We expect the same behavior to be present also in the cases of higher oligothiophenes, although our theoretical findings still await experimental confirmation for oligothiophenes containing more than four thiophene rings.

IV. Conclusions

The results reported in this paper for the series of oligothiophenes containing 2–6 thiophene rings by means of the combined DFT/TDDFT approach show quantitative or semi-quantitative agreement with the experimental spectra of the title molecules. The discrepancies may be attributed to separate reasons: (i) the experimental conditions involving the matrix environment that were not explicitly reflected in the calculations, (ii) the ground state saddle point corresponding to the enforced planar conformation of the oligothiophenes that might adversely affect the calculated normal modes or geometries, and (iii) the inherent imperfections of the applied DFT approach leading to

inadequate description of the excited state electron density and the excited state geometry. At present we are unable to tell which of the abovementioned factors dominates. Leaving aside the possible vibronic model refinements, especially for the high-frequency modes, we wish to suggest that too large delocalization of the calculated geometry differences due to the $1^1A_g(1^1A_1) \leftarrow 1^1B_u(1^1B_2)$ transition may be responsible for errors in the respective HR parameters. On the other hand, the low-frequency vibrations are most likely to be affected by neglecting the matrix environment in the calculations and by the enforced planarity of the molecules. For bithiophene it turned out that applying a larger basis set brought about a considerable improvement of the HR parameter for the lowest frequency totally symmetric normal mode. A detailed study of the actual importance of all the abovementioned sources of error is currently under way in our laboratory. However, the performance of the TDDFT method for calculating geometries of oligothiophenes in their lowest excited singlet state may be regarded as quite satisfactory. Moreover, the TDDFT methodology seems to behave properly not only for small but also for moderately large oligothiophenes. It is clear that the approach based on the TDDFT calculations has yet to be tested for other molecules that belong to different classes of compounds or different symmetry groups. Special care should be taken when tackling systems where the electronic excited state wave function contains substantial contributions of more than a single electronic configuration. In our opinion, the results obtained so far are quite encouraging. Therefore, we arrive at the conclusion that the HR parameters reported in this paper can be useful when studying vibronic effects in the molecular crystals of oligothiophenes, a subject that has recently been discussed by several research groups.^{33–35,54}

References and Notes

- (1) Ahlrichs, R.; Bär, M.; Häser, M.; Horn, H.; Kölmel, C. *Chem. Phys. Lett.* **1989**, *162*, 165.
- (2) Garnier, F.; Hajlaoui, R.; Yassar, A.; Srivastava, P. *Science* **1994**, *265*, 1684.
- (3) Dabalapur, A.; Torsi, L.; Katz, H. E. *Science* **1995**, *268*, 280.
- (4) Garnier, F.; Hajlaoui, R.; El Kassmi, A.; Horowitz, G.; Laire, L.; Porzio, W.; Armanini, M.; Provasoli, F. *Chem. Mater.* **1998**, *10*, 3334.
- (5) Friend, S. H. *Nature (London)* **1999**, *397*, 121.
- (6) Meng, H.; Bao, Z.; Lovinger, A. J.; Wang, B.; Muijsce, A. M. *J. Am. Chem. Soc.* **2001**, *123*, 9214.
- (7) Dimitrakopoulos, C. D.; Malenfant, P. R. L. *Adv. Mater.* **2002**, *14*, 99.
- (8) Becker, R. S.; de Melo, J. S.; Macanita, A. L.; Elisei, F. *J. Phys. Chem.* **1996**, *100*, 18683.
- (9) Kouki, F.; Spearman, P.; Vacat, P.; Horowitz, G.; Garnier, F. *J. Chem. Phys.* **2000**, *113*, 385.
- (10) DiCesare, N.; Belletete, M.; Garcia, E. R.; Leclerc, M.; Durocher, G. *J. Phys. Chem. A* **1999**, *103*, 3864.
- (11) Yang, A.; Kuroda, M.; Shiraiishi, Y.; Kobayashi, T. *J. Phys. Chem. B* **1998**, *102*, 3706.
- (12) Wasseberg, D.; Marsal, P.; Meskers, S.; Janssen, R.; Beljonne, D. *J. Phys. Chem. B* **2005**, *109*, 4410.
- (13) Chadwick, J.; Kohler, B. *J. Phys. Chem.* **1994**, *98*, 3631.
- (14) Negri, F.; Zgierski, M. *J. Chem. Phys.* **1994**, *100*, 2571.
- (15) Cornil, J.; Beljonne, D.; Bredas, J. L. *J. Chem. Phys.* **1995**, *103*, 842.
- (16) Colditz, R.; Grebner, D.; Helbig, M.; Rentsch, S. *Chem. Phys.* **1995**, *201*, 309.
- (17) Beljonne, D.; Cornil, J.; Friend, R. H.; Janssen, R.; Bredas, J. L. *J. Am. Chem. Soc.* **1996**, *118*, 6453.
- (18) Belletete, M.; DiCesare, N.; Leclerc, M.; Durocher, G. *Chem. Phys. Lett.* **1996**, *250*, 31.
- (19) Rubio, M.; Merchan, M.; Orti, E.; Roos, B. *J. Chem. Phys.* **1995**, *102*, 3580.
- (20) Rubio, M.; Merchan, M.; Orti, E.; Roos, B. *Chem. Phys. Lett.* **1996**, *248*, 321.
- (21) Duarte, H.; Dos Santos, H.; Rocha, D. O. S.; De Almeida, W. *J. Chem. Phys.* **2000**, *113*, 4206.

- (22) Telesca, R.; Bolink, H.; Yunoki, S.; Hadziioannou, G.; Th, P.; Snijders, J. G.; Jonkman, H. T.; Savatzky, G. A. *Phys. Rev. B* **2001**, *63*, 155112.
- (23) Salzner, U. *J. Chem. Theory Comput.* **2007**, *3*, 1143.
- (24) Rubio, M.; Merchan, M.; Pou-Amerigo, R.; Orti, E. *ChemPhysChem* **2003**, *4*, 1308.
- (25) Andruniow, T.; Zborowski, K.; Pawlikowski, M. *Chem. Phys. Lett.* **1996**, *259*, 193.
- (26) Hazra, A.; Nooijen, M. *Int. J. Quantum Chem.* **2003**, *95*, 643.
- (27) Sterzel, M.; Pilch, M.; Pawlikowski, M. T.; Skowronek, P.; Gawronski, J. *Chem. Phys. Lett.* **2002**, *362*, 243.
- (28) Sterzel, M.; Andrzejak, M.; Pawlikowski, M. T.; Gawronski, J. *Chem. Phys.* **2004**, *300*, 93.
- (29) Makowski, M.; Pawlikowski, M. T. *Int. J. Quantum Chem.* **2005**, *104*, 589.
- (30) Birnbaum, D.; Kohler, B. *J. Chem. Phys.* **1989**, *90*, 3506.
- (31) Birnbaum, D.; Kohler, B. *J. Chem. Phys.* **1991**, *95*, 4783.
- (32) Birnbaum, D.; Fichou, D.; Kohler, B. *J. Chem. Phys.* **1992**, *96*, 165.
- (33) Petelenz, P.; Andrzejak, M. *J. Chem. Phys.* **2000**, *113*, 11306.
- (34) Zhao, Z.; Spano, F. C. *J. Chem. Phys.* **2005**, *122*, 114701.
- (35) Spano, F. C.; Silvestri, L.; Spearman, P.; Raimondo, L.; Tavazzi, S. *J. Chem. Phys.* **2007**, *127*, 184703.
- (36) Pelletier, M.; Brisse, F. *Acta. Crystallogr.* **1994**, *C50*, 1942.
- (37) van Bolhuis, F.; Wynberg, H.; Havinga, E.; Meijer, E.; Staring, E. *Synth. Met.* **1989**, *30*, 381.
- (38) Horowitz, *Chem. Mater.* **1995**, *7*, 1337.
- (39) Porzio, W.; Destri, S.; Maschera, M.; Brückner, S. *Acta Polym.* **1993**, *44*, 266.
- (40) Siegrist, T.; Kloc, C.; Laudise, R. A.; Katz, H. E.; Haddon, R. C. *Adv. Mater.* **1998**, *10*, 379.
- (41) De Oliveira, M.; Duarte, H.; Pernaut, J.-M.; De Almeida, W. J. *Phys. Chem. A* **2000**, *104*, 8256.
- (42) Siebrand, W.; Zgierski, M. Z. *J. Chem. Phys.* **1979**, *71*, 3561.
- (43) Schäfer, A.; Huber, C.; Ahlrichs, R. *J. Chem. Phys.* **1994**, *100*, 5829.
- (44) Weigend, F.; Köhn, A.; Hättig, C. *J. Chem. Phys.* **2002**, *116*, 3175.
- (45) Vosko, S.; Wilk, L.; Nussair, M. *Can. J. Phys.* **1980**, *58*, 1200.
- (46) Becke, A. D. *Phys. Rev. A* **1988**, *38*, 3098.
- (47) Perdew, J. P. *Phys. Rev. B* **1986**, *33*, 8822.
- (48) Lee, C.; Yang, W.; Parr, R. G. *Phys. Rev. B* **1988**, *37*, 785.
- (49) Becke, A. D. *J. Chem. Phys.* **1993**, *98*, 5648.
- (50) Karlström, G.; Lindh, R.; Malmqvist, B.-Å.; Roos, B. O.; Ryde, U.; Veryazov, V.; Widmark, P.-O.; Cossi, M.; Schimmlpfennig, B.; Neogrady, P.; Seijo, L. *Comput. Mater. Sci.* **2003**, *28*, 222.
- (51) Pierloot, K.; Dumek, B.; Widmark, P.-O.; Roos, B. O. *Theor. Chim. Acta* **1995**, *90*, 87.
- (52) Szegalmi, A.; Engel, V.; Zgierski, M.; Popp, J.; Schmitt, M. *J. Raman. Spectrosc.* **2006**, *37*, 148.
- (53) Makowski, M.; Pawlikowski, M. T. *J. Chem. Phys.* **2003**, *24*, 12795.
- (54) Meinardi, F.; Cerminara, M.; Blumstengel, S.; Sasella, A.; Borghesi, A.; Tubino, R. *Phys. Rev. B* **2003**, *67*, 184205.

JP807752K